

The Role of Barrier Layer in Southeastern Arabian Sea During the Development of Positive Indian Ocean Dipole Events

GUO Feiyan¹⁾, LIU Qinyu^{1)*}, ZHENG Xiao-Tong¹⁾, and SUN Shan²⁾

1) Physical Oceanography Laboratory and Key Laboratory of Ocean-Atmosphere Interaction and Climate in Universities of Shandong, Ocean University of China, Qingdao 266100, P. R. China

2) NOAA Earth System Research Laboratory, 325 Broadway, Boulder, Colorado 80305, USA

(Received October 11, 2012; revised November 26, 2012; accepted February 5, 2013)

© Ocean University of China, Science Press and Springer-Verlag Berlin Heidelberg 2013

Abstract Using data from Argo and simple ocean data assimilation (SODA), the role of the barrier layer (BL) in the southeastern Arabian Sea (SEAS: 60°E–75°E, 0°–10°N) is investigated during the development of positive Indian Ocean Dipole (IOD) events from 1960 to 2008. It is found that warmer sea surface temperature (SST) in the northern Indian Ocean appears in June in the SEAS. This warm SST accompanying anomalous southeastern wind persists for six months and a thicker BL and a corresponding thinner mixed layer in the SEAS contribute to the SST warming during the IOD formation period. The excessive precipitation during this period helps to form a thicker BL and a thinner mixed layer, resulting in a higher SST in the SEAS. Warm SST in the SEAS and cold SST to the southeast of the SEAS intensify the southeasterly anomaly in the tropical Indian Ocean, which transports more moisture to the SEAS, and then induces more precipitation there. The ocean-atmosphere interaction process among wind, precipitation, BL and SST is very important for the anomalous warming in the SEAS during the development of positive IOD events.

Key words sea surface temperature (SST); mixed layer; barrier layer; Indian Ocean Dipole (IOD); persistence; precipitation; southeastern Arabian Sea

1 Introduction

The variability associated with sea surface temperature (SST), wind and precipitation in the tropical Indian Ocean has been identified and defined as the Indian Ocean Dipole (IOD) mode (Saji *et al.*, 1999; Webster *et al.*, 1999; Murtugudde *et al.*, 2000; Yamagata *et al.*, 2003; Luo *et al.*, 2010; Zheng *et al.*, 2010). The Indian Ocean Dipole mode displays an anomalous east-west SST gradient and is accompanied with wind and precipitation anomalies in the tropical Indian Ocean, so it is also referred to as the Indian Ocean zonal mode (Le Blanc and Boulanger, 2001; Huang and Kinter, 2002). During Indian Ocean Dipole events, the changes in SST are found to be closely associated with changes in surface wind, the equatorial wind reverses direction from westerlies to easterlies, and changes in sea surface wind are associated with a basin-wide anomalous Walker circulation (Yamagata *et al.*, 2002). According to previous studies, the Bjerknes-type (Bjerknes, 1969) feedback (Saji *et al.*, 1999; Li *et al.*, 2003), the wind-evaporation-SST feedback (Wang *et al.*, 2003; Li *et al.*, 2003; Halkides *et al.*, 2006) and the oceanic Rossby waves (Webster *et al.*, 1999; Xie *et al.*, 2002;

Huang and Kinter, 2002) are dominant mechanisms for the development of IOD events.

During an IOD event, the SST in the Indian Ocean experiences large changes. Saji *et al.* (1999) analyzed six extreme events to present the life cycle of a typical dipole mode event. According to their studies, the northern Indian Ocean gets unusually warm in the initial development of a positive IOD event. Previous studies mainly discussed the SST cooling in the tropical southeastern Indian Ocean and the SST warming in the equatorial southwestern Indian Ocean during an IOD formation. So far it is still not very clear why the warm SST appears in the northwest Indian Ocean like the one in the southeastern Arabian Sea (SEAS: 60°E–75°E, 0°–10°N), why there is a corresponding southeasterly wind anomaly during the entire formation process of an IOD event, and whether there are other physical mechanisms contributing to the SST anomaly in the SEAS in addition to the wind-thermocline-SST feedback, wind-evaporation-SST feedback, and ocean Rossby wave feedback mechanisms.

The intermediate layer between the bottom of mixed layer (ML) and the top of the thermocline is called the barrier layer (BL) (Godfrey and Lindstrom, 1989; Lukas and Lindstrom, 1991; Chu *et al.*, 2002). The excessive precipitation, river runoff and redistribution of the low-salinity water by advection are in favor of the presence of BL. In the SEAS, the existence of the BL has been re-

* Corresponding author. Tel: 0086-532-66782556

E-mail: liuqy@ouc.edu.cn

ported by several earlier studies. The winter monsoon current brings the low-salinity and low-temperature water from the Bay of Bengal into the SEAS (Shetye *et al.*, 1991; Rao and Sivakumar, 2003; Sharma *et al.*, 2010), which is considered to contribute to the formation of a BL with shallow salinity and density stratification and an inversion layer (Thadathil and Gosh, 1992; Shenoi *et al.*, 1999). The heaviest precipitation on the eastern side of the Bay of Bengal and the Arabian Sea (Xie *et al.*, 2006) is also favorable for the formation of BL.

The BL thickness (BLT) is an important factor influencing the SST anomaly, as the thicker BL helps keeping the heat in the shallow mixed layer, leading to an increase in SST (Lewis *et al.*, 1990; Vialard and Delecluse, 1998a, b). In addition, the existence of a thick BL prevents the mixed layer from reaching the thermocline, suppresses the sub-surface cold water from getting into the surface layer and thus inhibits the surface cooling (Vialard and Delecluse, 1998a; Han *et al.*, 2001; Annamalai *et al.*, 2003; Qiu *et al.*, 2012). The formation and development of a BL in the SEAS also play an important role for SST variation in Arabian Sea (Shenoi *et al.*, 2004; Durand *et al.*, 2004). Masson *et al.* (2005) showed that the existence of BL and the subsurface inversion in the SEAS substantially contribute to the SST increase and the early onset of the south-west monsoon. Using an ocean general circulation model (OGCM), De Boyer Montégut *et al.* (2007) found that heat accumulated in the barrier layer in the eastern Arabian Sea can warm the surface layer by 0.4°C . In this study, it is proposed that the warm SST is important to maintain the southeasterly wind anomaly in the tropical Indian Ocean during the formation of a positive IOD, and there is an interannual variation of BL in the SEAS, which contributes to the anomalous warm SST in this region.

Using Argo and SODA datasets the role of BL in the positive IOD is discussed in this paper as organized as follows. Section 2 introduces the data used in the study. Section 3 proposes the role of the BL during the development of the IOD event and discusses the warm SST and precipitation anomaly in the SEAS. The summary is in Section 4.

2 Data

In the present study, the monthly mean wind at 10 m and surface heat flux from the NCEP/NCAR reanalysis products are adopted. This dataset has a spatial resolution of $1.875^{\circ}\times 1.904^{\circ}$ and covers the period from 1950 to 2010. The monthly mean global precipitation dataset, Precipitation Reconstruction (Chen *et al.*, 2003), is used to examine the rainfall changes in the ocean, which is constructed on a $2.5^{\circ}\times 2.5^{\circ}$ horizontal grid over the globe for the period from 1948 to the present.

The upper-level ocean temperature and salinity are needed to study the developmental process of the positive IOD events. Among many available products, the monthly mean data from the simple ocean data assimilation (SODA, v2.2.4) are selected for this study. The hori-

zontal resolution of the dataset is $0.5^{\circ}\times 0.5^{\circ}$ and the vertical resolution is 10 m in the upper-level (a total of 40 vertical layers, Carton and Giese, 2008). The wind data used to force this version of SODA are from the 20th Century Atmospheric Reanalysis products (Compo *et al.*, 2011), which compare well with the NCEP/NCAR reanalysis, which is also used here, for both are based on surface observations and the NCEP Global Forecast System. The adequacy of using SODA data to study the Indian Ocean coupled dynamics is discussed in Xie *et al.* (2002). In addition, the temperature and salinity profiles from Argo floats are used to investigate the IOD event in 2006. The Argo data have a $1^{\circ}\times 1^{\circ}$ horizontal resolution and were collected from 2005 to 2010.

Because the IOD dominates the SST interannual variability, the decadal/interdecadal components are removed through band-pass filters and only the signals of interannual variability (13–84 months) are retained in order to extract the useful information related to IOD.

3 The Role of the Barrier Layer

The SST anomaly presents a positive IOD event as an east (cold) to west (warm) dipole mode. In Saji *et al.* (1999), the warm SST anomaly exists in the SEAS during the development of the positive IOD events. In this study the 7-year Argo and 49-year SODA data are used to illustrate the impact of the BL anomaly on the anomalous warm SST in the SEAS. The warm SST in the SEAS and cold SST to the southeast of the SEAS induce the southeasterly wind anomaly. This process plays an important role in the development of the IOD events.

3.1 Persistence of SST Anomaly in the SEAS

Based on the IOD index defined by Saji *et al.* (1999), the standard deviation of SST difference between the western and eastern equatorial Indian Ocean should be larger than 1.5 as IOD composite cases are identified. Based on this criteria, seven strong positive IOD events occurred in 1961, 1967, 1972, 1982, 1994, 1997 and 2006, respectively (Fig.1). Compared with the IOD cases in Saji *et al.*'s study (1999), the 2006 IOD event is the first strong IOD event since Argo floats were fully deployed in the Indian Ocean. Fig.2 shows the evolution of SST and sea surface wind anomalies in 2006, together with the composite results associated with the seven IOD events indicated in Fig.1. Only statistically significant results with a confidence level exceeding 90% are shown in Figs.2d, 2e and 2f. For all seven IOD years, an anomalous warm SST occurs in the SEAS during June–July, and stays there for the next several months, accompanied with southeasterly winds. A noticeable difference is that warm SST in the 2006 IOD year is also observed in the central southern Indian Ocean (Fig.2). Chowdary *et al.* (2009) found that a thick barrier layer propagating with the pronounced westward Rossby waves potentially contributed to this warming in the SEAS. According to the composite results of SST, the SEAS is defined as the crucial region

in this study, most of which is within the western pole of IOD defined by Saji *et al.* (1999). The SST anomalies and the northwest-to-southeast dipole pattern, formed by the anomalous warming in the SEAS and cooling in the southeastern tropical Indian Ocean, are similar when comparing the results with the Argo data (left column) and the SODA data (right column) in Fig.2. The SST patterns from SODA are also similar to those from the Met Office Hadley Centre's sea ice and sea surface temperature dataset (HadISST1). To ensure the credibility of the Argo

and SODA data used here, the SST patterns in the four strong IOD events (1982, 1994, 1997, and 2006) are further verified by using the daily data of the optimum interpolation sea surface temperature version 2 (OISST.V2) from 1981 to the present (Reynolds *et al.*, 2002). Such a SST pattern during the early development of IOD results in strong southeasterly wind anomaly and the corresponding upwelling in the southeastern tropical Indian Ocean. As the anomalous warm SST extends westward and southward starting from August the anomalous

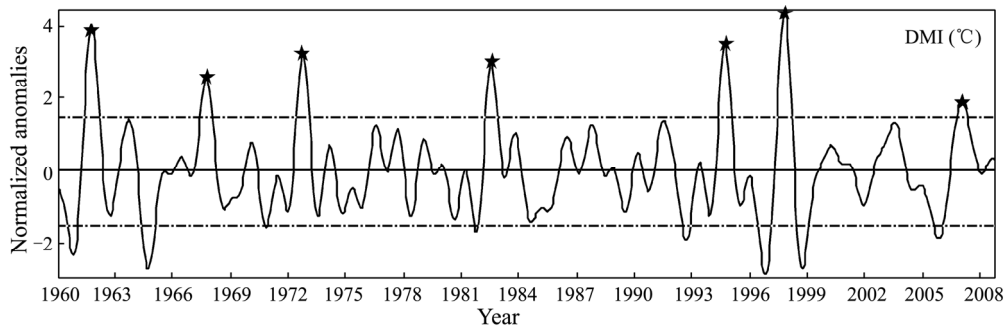


Fig.1 Time evolution of the normalized Indian Ocean Dipole mode index (DMI in $^{\circ}\text{C}$). The star marks the IOD year.

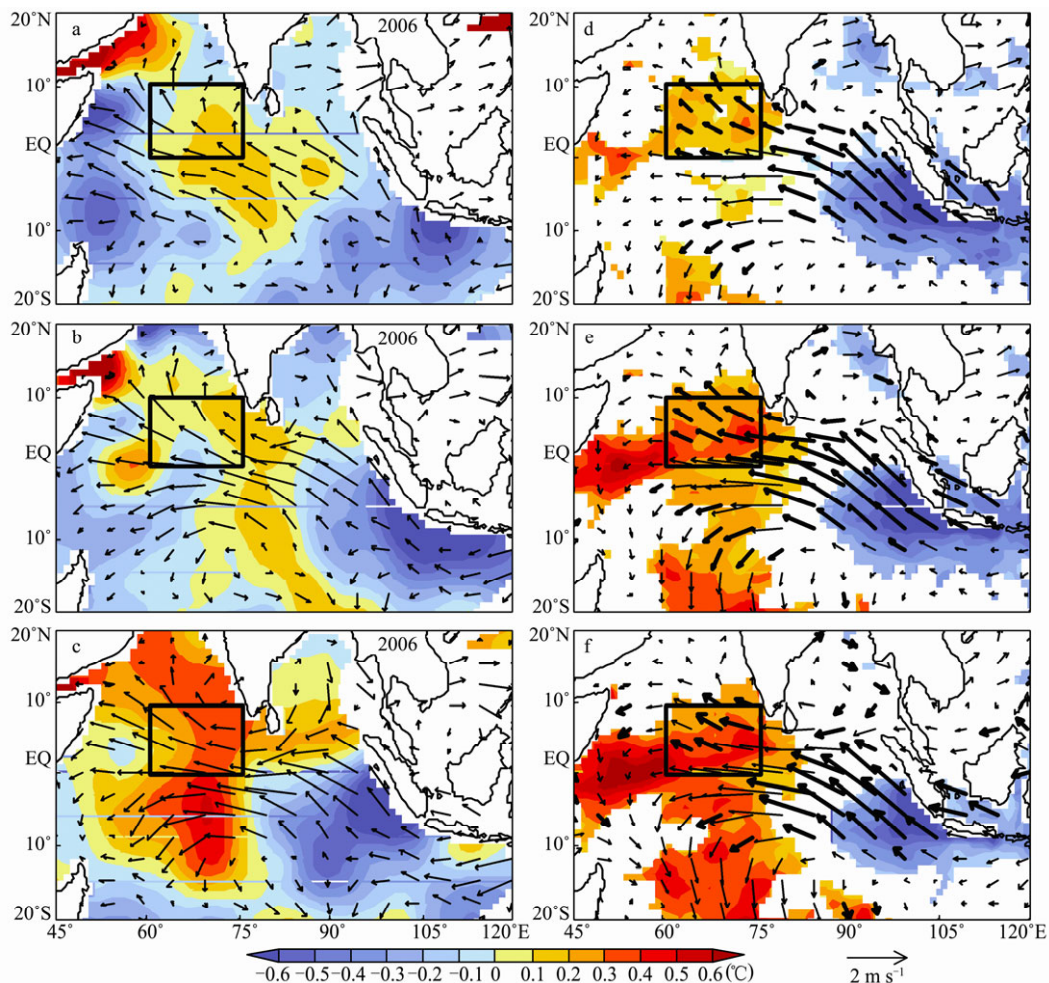


Fig.2 The 2006 SST anomaly (shaded in $^{\circ}\text{C}$) and sea surface wind anomaly (arrows in m s^{-1}) fields from (a) June–July, (b) August–September and (c) October–November based on the Argo data. The same are shown in (d) to (f) for the composites of all seven positive IOD events based on SODA. The statistical significance of the analyzed anomalies is estimated by *t*-test. Anomalies of SST and surface wind exceeding 90% significance level are shown by the color shading and arrow, respectively. The black box indicates the crucial region in SEAS (0° – 10°N , 60°E – 75°E).

southeasterly winds are further strengthened. The existence of warm SST anomaly in the SEAS plays a crucial role in enhancing the anomalous southeasterlies in the southeastern tropical Indian Ocean and the equatorial region. Next the mechanisms to maintain the warming in the SEAS will be investigated.

3.2 The Role of the Barrier Layer in the SEAS

In order to understand how the BL maintains the warm SST anomaly in the SEAS, the BLT is calculated as the difference between the isothermal layer depth and the MLD, where the isothermal layer depth is defined as the depth at which temperature is 0.5 °C lower than SST (Monterey and Levitus, 1997), and the MLD is the depth where water density is 0.125 kg m⁻³ higher than that at the sea surface (Levitus, 1982; Huang and Qiu, 1994). A vertical linear interpolation is adopted due to the insufficient vertical resolution of SODA data, where either the MLD or isothermal layer depth lies between two standard levels. Using Argo floats data from 2005 to 2010 and SODA data from 1960 to 2008, the climatology mean of BLT and the standard deviation in the tropical Indian Ocean during June–November are calculated and shown in Fig.3. From both datasets, a thicker BL exists in the southeastern tropical Indian Ocean, the Bay of Bengal, and the Arabian Sea, although the Argo data shows a mean BLT of 10 m and the SODA data shows a BLT of 5 m in the SEAS. The variation of BLT in the SEAS is significant and is almost equal to its climatology mean. The temperature and salinity from SODA compares well with those from the Argo data.

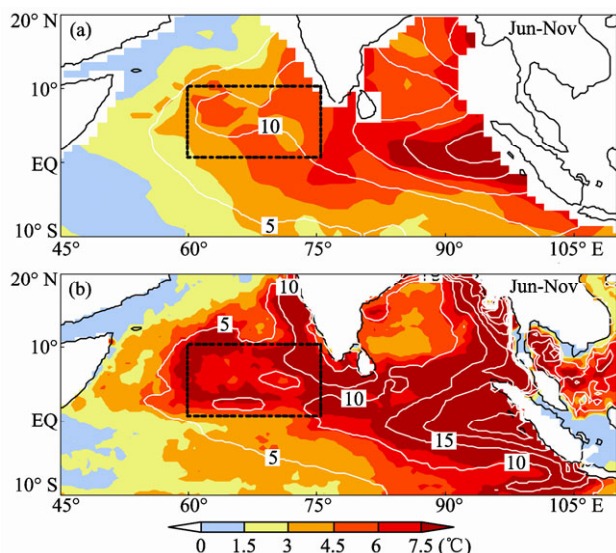


Fig.3 Barrier layer thickness (contours in m) and its standard deviation (color shading in m) in June–November based on (a) Argo data averaged from 2005 to 2010 and (b) SODA averaged from 1960 to 2008. The crucial region in SEAS (0°–10°N, 60°E–75°E) is outlined by dashed line.

Previous studies (Annamalai *et al.*, 2003; Masson *et al.*, 2005) have examined the warming effect of BL on SST in the Indian Ocean. Here it is proposed that the variation of

the BLT may influence the SST anomaly in the SEAS. In order to confirm the hypothesis, the mixed layer temperature equation is considered (*e.g.*, Qiu, 2000; Liu *et al.*, 2005):

$$\frac{\partial T_m}{\partial t} = Q_{net} / \rho c_p h_m - V_m \cdot \nabla T_m - w_e (T_m - T_d) / h_m \quad (1)$$

Using the perturbation method, Eq. (1) can be written as:

$$\begin{aligned} \frac{\partial T'_m}{\partial t} = & \left(-\frac{\bar{Q}_{net}}{c_p \rho \bar{h}_m^2} + \frac{\bar{w}_e (\bar{T}_m - \bar{T}_d)}{\bar{h}_m} \right) h'_m + \\ & \frac{Q'}{c_p \rho \bar{h}_m} - (V'_m \cdot \nabla \bar{T}_m + \bar{V}_m \cdot \nabla T'_m) - \\ & \left(\frac{w'_e (\bar{T}_m - \bar{T}_d)}{\bar{h}_m} + \frac{\bar{w}_e (T'_m - T'_d)}{\bar{h}_m} \right) \end{aligned} \quad (2)$$

Among the four terms on the right hand side of Eq. (2), the first term is the contribution of MLD anomaly to the SST variation anomaly; the second, third, and fourth terms are the contributions of the net air–sea heat flux anomaly, the current anomaly and horizontal gradient of SST anomaly, and the vertical velocity anomaly and vertical temperature gradient anomaly, respectively. ρ and c_p in the equation are the sea water density and specific heat at constant pressure, respectively; \bar{Q}_{net} is the mean net air–sea heat flux; \bar{V}_m is the mean current velocity vertically averaged over the mixed layer, which is composed of surface geostrophic current and Ekman flow; w_e is the mean entrainment velocity; \bar{h}_m is the mean mixed layer depth; \bar{T}_m is the mean temperature in the mixed layer; \bar{T}_d is the mean temperature beneath the mixed layer; Q'_{net} , V'_m , h'_m , T'_m , w'_e , T'_d are the respective anomalies.

The four terms averaged over the SEAS for each month in 2006 are shown in Fig.4a. Among those terms, the first term is the largest, except in June, and reaches its maximum (0.33 °C mon⁻¹) in October (Figs.4a, and 4b), and the fourth term is the smallest and can be neglected. The large values of the first term indicate that the positive SST anomaly mainly comes from the contribution of negative MLD anomaly, for a thinner mixed layer has a lower heat capacity. In general, the contribution of negative MLD anomaly (the first term) is dominant in the SST warming during the development period of the positive IOD in 2006. Corresponding to the negative MLD anomalies, there are positive BLT anomalies (Fig.4b).

The composite of each of the four terms during the seven positive IOD events is shown in Fig.4c. The above discussion on the 2006 Argo data applies to these positive IOD events as well: the positive SST anomaly in the SEAS is mainly due to the contribution of negative MLD anomaly in Fig.4d, where it shows the corresponding positive BLT anomaly, and the absolute values of the BLT are almost the same as the absolute MLD anomaly in the composite results. Because the MLD decreases by about

15%–20% from its climatology, the effect of net air–sea heat flux on the SST is amplified, for a thinner ML has a lower heat capacity. The net heat flux reanalysis from NCEP compares well with the objectively analyzed air–sea fluxes (OAFlux, Praveen-Kumar *et al.*, 2012) and OAFlux (Yu *et al.*, 2008). Corresponding to both for the 2006 IOD event and the composite of seven IOD events,

the MLD shows negative anomalies, while the BLT positive anomalies. A shallower ML is the main mechanism for the persistence of positive SST anomalies in the SEAS during the IOD formation period. Morioka *et al.* (2010, 2011) pointed out the importance of the MLD in SST anomaly and the findings here are consistent with their results.

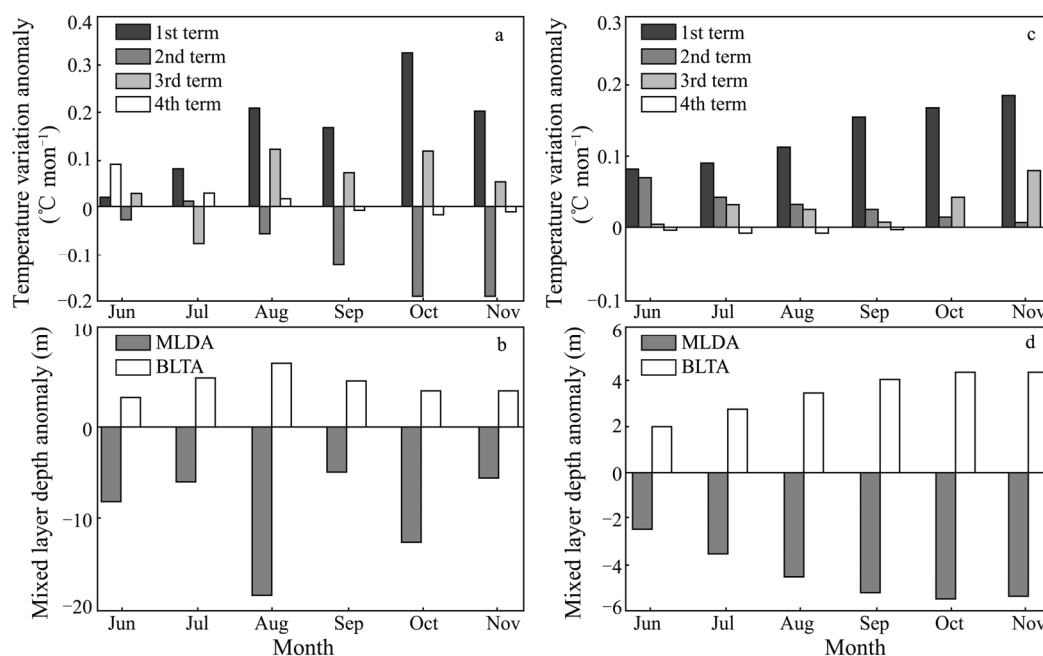


Fig.4 (a) The temperature variation anomaly ($^{\circ}\text{C mon}^{-1}$), including the MLD anomaly (1st term, dark bar), the sea surface net heat flux anomaly (2nd term, dark gray bar), the current anomaly and the horizontal gradient of SST anomaly (3rd term, light gray bar), and the vertical velocity anomaly and vertical temperature gradient anomaly (4th term, white bar); (b) The mixed layer depth anomaly (MLDA in m, dark gray bar) and the barrier layer thickness anomaly (BLTA in m, white bar) averaged in the SEAS (0° – 10°N , 60°E – 75°E) from June to November. (a) and (b) are based on the 2006 Argo data; (c) and (d) show the same variables as (a) and (b), respectively, for the composite of seven positive IOD events from SODA.

3.3 The Ocean-Atmosphere Interaction Processes Among Wind, Precipitation, BL, and SST in the SEAS

In the tropics, the BL usually appears as a low-salinity water layer between isothermal layer and ML after heavy precipitation or low-salinity advection from other areas. The results of the NCEP/NCAR reanalysis precipitation indicate that the positive precipitation anomaly begins to appear in the SEAS in August and becomes larger gradually afterward (Figs.5b to 5c). A composite of precipitation anomaly appearing in the seven IOD years (Figs.5d to 5f) shows that in the positive IOD events the precipitation has a positive anomaly in the SEAS in June–July and this anomaly increases in magnitude with time, which agrees well with changes in SST (Fig.2) and BLT (Fig.4d). Opposite to the heavy precipitation in the SEAS, the precipitation reduces greatly in the eastern Indian Ocean from June to November. The precipitation pattern of the four strong IOD events (1982, 1994, 1997 and 2006) agrees well with the Global Precipitation Climatology Project version 2 (GPCP.V2.2) combined precipitation data set (Adler *et al.*, 2003). The positive precipitation

anomaly is important for a positive anomaly of the BLT in the SEAS. Other studies also show that fresh water coming from the Bay of Bengal is important for salinity budget in the SEAS (Jensen, 1991; Shetye *et al.*, 1991; Shenoi *et al.*, 1999; Rao and Sivakumar, 1999, 2003).

In order to examine the relationships among precipitation, SST, BL and MLD, the normalized time series of September–November precipitation anomaly (PreA), SST anomaly (SSTA), BLT anomaly (BLTA) and MLD anomaly (MLDA) are averaged in the SEAS from 1960 to 2008 and are shown in Fig.6. The PreA is strongly correlated with BLTA during the peak IOD period (September–November), with a positive correlation coefficient of 0.75 and a significance level exceeding 95%. This strong correlation further indicates that more precipitation will increase the thickness of BL. Corresponding to the thicker BL, the shoaling of ML will warm the SST based on the early discussion. It is also found that warm SST could in turn increase the BLT. The relationship between SSTA and BLA (MLDA) is examined and the correlation coefficient between them is 0.47 (–0.48) with a significance level exceeding 95%. Warm SST in the SEAS and cold SST in the southeastern tropical Indian Ocean form an SST gradient, which provides a favorable condition for

the occurrence of the anomalous southeasterly winds (Fig.2). The winds can bring abundant moisture from the southeastern Indian Ocean, and enhance the precipitation. The correlation coefficient between SSTA and PreA is 0.46 with a confidence level of 95%. The excessive precipitation results in the BL thickening and the ML shoaling. The correlation coefficients between the four variables and the IOD index of SON are 0.79, 0.72, 0.68 and -0.47 with a significance level exceeding the 95%,

respectively, indicating a close relationship between those variables and the IOD event. Saji *et al.* (1999) pointed out the great changes of zonal wind over the equatorial central and eastern Indian Ocean during the IOD events. Our results further illustrate that there is an ocean-atmosphere interaction process in the SEAS among SST, wind, precipitation, BL, and ML during a positive IOD event. Along with other mechanisms the BL plays an important role in the development of IOD.

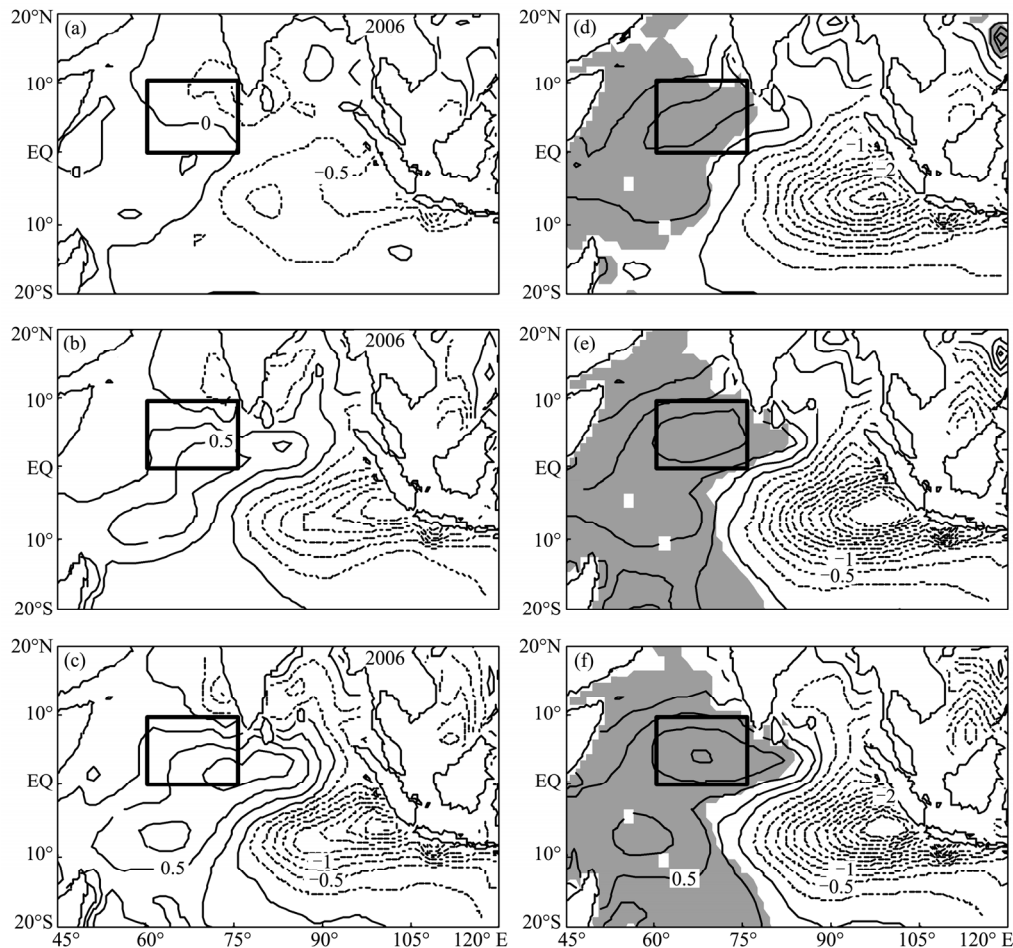


Fig.5 The precipitation anomaly fields (contours in mm d^{-1}) in (a) June–July, (b) August–September and (c) October–November using the 2006 Argo data. The same fields are shown in (d)–(f) for the composite of seven positive IOD events from SODA and the shaded area has a significance level exceeding 90%. The box indicates the crucial region in SEAS (0° – 10° N, 60° E– 75° E).

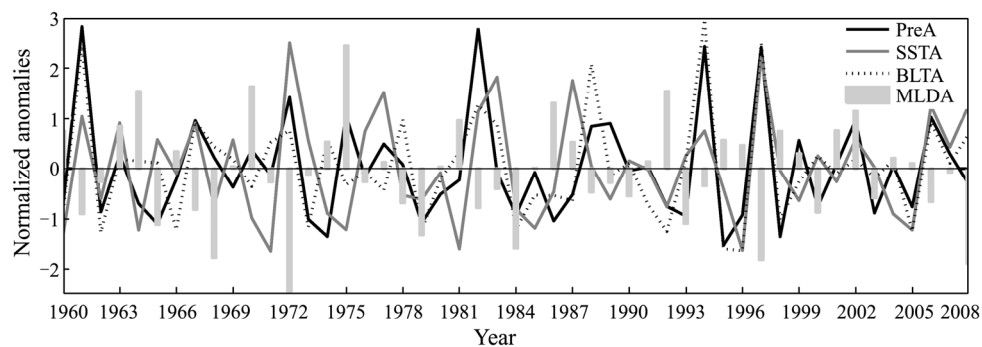


Fig.6 The normalized time series of the precipitation anomaly (PreA, black solid line), sea surface temperature anomaly (SSTA, gray solid line), barrier layer thickness anomaly (BLTA, dashed line), and mixed layer depth anomaly (MLDA, gray bar) averaged in the SEAS in September–November.

4 Summary and Discussion

Using data from the Argo floats and SODA reanalysis, the composite analysis is conducted to investigate the development processes of positive IOD events. It is found that warmer SST appears in June–July in the SEAS (0° – 10° N, 60° E– 75° E), most of which is in the western pole of the IOD defined by Saji *et al.* (1999). This anomalous warm SST extends westward and southward, and can persist for several months. The positive temperature anomaly in the SEAS is mainly due to the MLD decrease (the first term in the mixed layer temperature equation), especially from August to November. Because the MLD is about 15%–20% thinner comparing with its climatology, the effect of net air–sea heat flux on the SST is amplified, for a thinner ML has a lower heat capacity. The contribution of net heat flux (the second term) and the total contribution of the current anomaly and horizontal gradient of SST anomaly (the third term) are positive in some months but are smaller than the contribution of the MLD anomaly (the first term). The total contribution of vertical velocity anomaly and vertical temperature gradient anomaly (the fourth term) is so small that their effect is negligible.

It is shown that ML and BL are important in adjusting ocean–atmosphere interactions and thus affecting weather and climate. Warming in the SEAS caused by the thickening of BLT (shoaling of MLD) enhances the precipitation and increases the southeast–northwest SST gradient with the cold SST in the southeastern Indian Ocean. The large SST gradient intensifies the anomalous southeasterly winds, which brings more moisture to the SEAS. The excessive precipitation reduces the salinity, increases the stratification near the surface, and leads to a decrease in MLD and an increase in BLT, which then contributes to a warmer SST in the SEAS. This ocean–atmosphere interaction process among wind, precipitation, BL and SST plays an important role during the development of positive IOD events in the SEAS.

Acknowledgements

Comments by the two anonymous reviewers greatly helped improve the manuscript. Thanks to Profs. S.-P. Xie and W. Han for their comments on the manuscript. Argo data were collected and made available by the International Argo Program of the Global Ocean Observing System (<http://www.argo.ucsd.edu>, <http://argo.jcommops.org>). This study is supported by the National Basic Research Program of China (2012CB955602), Ministry of Science and Technology of China (National Key Program for Developing Basic Science 2010CB428904), the NSFC (41176006, 40921004, 41106010), and the 111 Project of China (Program of Introducing Talents of Discipline to Universities No. B07036).

References

Adler, R. F., Huffman, G. J., Chang, A., Ferraro, R., Xie, P.,

- Janowiak, J., Rudolf, B., Schneider, U., Curtis, S., Bolvin, D., Gruber, A., Susskind, J., and Arkin, P., 2003. The Version 2 global precipitation climatology project (GPCP) monthly precipitation analysis (1979–present). *Journal of Hydrometeorology*, **4**: 1147–1167.
- Annamalai, H., Murtugudde, R., Potemra, J., Xie, S., Liu, P., and Wang, B., 2003. Coupled dynamics over the Indian Ocean: Spring initiation of the zonal mode. *Deep-Sea Research II*, **50**: 2305–2330.
- Bjerknes, J., 1969. Atmospheric teleconnections from the equatorial Pacific. *Monthly Weather Review*, **97**: 163–172.
- Carton, J. A., and Giese, B. S., 2008. A reanalysis of ocean climate using simple ocean data assimilation (SODA). *Monthly Weather Review*, **136**: 2999–3017.
- Chen, M., Xie, P., Janowiak, J. E., Arkin, P. A., and Smith, T. M., 2003. Reconstruction of the oceanic precipitation from 1948 to the present. *The AMS 14th Symposium on Global Changes and Climate Variations*. American Meteorological Society, Long Beach, CA.
- Chowdary, J. S., Gnanaseelan, C., and Xie, S.-P., 2009. Westward propagation of barrier layer formation in the 2006–07 Rossby wave event over the tropical southwest Indian Ocean. *Geophysical Research Letters*, **36**, L04607, DOI: 10.1029/2008GL036642.
- Chu, P. C., Liu, Q., Jia, Y., and Fan, C., 2002. Evidence of a Barrier Layer in the Sulu and Celebes Seas. *Journal of Physical Oceanography*, **32** (11): 3299–3309.
- Compo, G. P., Whitaker, J. S., Sardeshmukh, P. D., Matsui, N., Allan, R. J., Yin, X., Gleaso B. E., Vose, R. S., Rutledge, G., Bessemoulin, P., Brönnimann, S., Brunet, M., Crouthamel, R. I., Grant, A. N., Groisman, P. Y., Jones, P. D., Kruk, M. C., Kruger, A. C., Marshall, G. J., Maugeri, M., Mork, H. Y., Nordli, Ø., Ross, T. F., Trigo, R. M., Wang, X. L., Woodruff, S. D., and Worley, S. J., 2011. The twentieth century reanalysis project. *Quarterly Journal of the Royal Meteorological Society*, **137**: 1–28, DOI: 10.1002/qj.776.
- De Boyer Montégut, C., Vialard, J., Shenoi, S. S. C., Shankar, D., Durand, F., Ethé, C., and Madec, G., 2007. Simulated seasonal and interannual variability of mixed layer heat budget in the northern Indian Ocean. *Journal of Climate*, **20**: 3249–3268, DOI: 10.1175/JCLI4148.1.
- Durand, F., Shetye, S. R., Vialard, J., Shankar, D., Shenoi, S. S. C., Ethé, C., and Madec, G., 2004. Impact of temperature inversions on SST evolution in the south-eastern Arabian Sea during the pre-summer monsoon season. *Geophysical Research Letters*, **31**, L01305, DOI: 10.1029/2003GL018906.
- Godfrey, J. S., and Lindstrom, E. J., 1989. The heat budget of the equatorial western Pacific surface mixed layer. *Journal of Geophysical Research*, **94**: 8007–8017.
- Halkides, D. J., Han, W., and Webster, P. J., 2006. Effects of the seasonal cycle on the development and termination of the Indian Ocean Zonal Dipole Mode. *Journal of Geophysical Research*, **111**, C12017, DOI: 10.1029/2005JC003247.
- Han, W., McCreary, J. P., and Kohler, K. E., 2001. Influence of precipitation–evaporation and Bay of Bengal rivers on dynamics, thermodynamics, and mixed layer physics in the upper Indian Ocean. *Journal of Geophysical Research*, **106**: 6895–6916.
- Huang, B., and Kinter III, J. L., 2002. Interannual variability in the tropical Indian Ocean. *Journal of Geophysical Research*, **107**, 3199, DOI: 10.1029/2001JC001278.
- Huang, R. X., and Qiu, B., 1994. Three-dimensional structure of the wind-driven circulation in the subtropical North Pacific. *Journal of Physical Oceanography*, **24**: 1608–1622.
- Jensen, T. G., 1991. Modeling the seasonal undercurrents in the

- Somali Current system. *Journal of Geophysical Research*, **96** (C12): 22151-22167, DOI: 10.1029/91JC02383.
- Le Blanc, J. L., and Boulanger, J. P., 2001. Propagation and reflection of long equatorial waves in the Indian Ocean from TOPEX/POSEIDON data during the 1993–1998 period. *Climate Dynamics*, **17**: 547-557.
- Levitus, S., 1982. *Climatological Atlas of the World Ocean*. National Oceanic and Atmospheric Administration. NOAA Professional Paper-13, 173pp.
- Lewis, M. R., Carr, M., Feldman, G., Esaias, W., and Mc-Clain, C., 1990. Influence of penetrating solar radiation on the heat budget of the equatorial Pacific Ocean. *Nature*, **347**: 543-544.
- Li, T., Wang, B., Chang, C. P., and Zhang, Y., 2003. A theory for the Indian Ocean Dipole–zonal mode. *Journal of the Atmospheric Sciences*, **60**: 2119-2135.
- Liu, Q., Xie, S. P., Li, L., and Maximenko, N. A., 2005. Ocean thermal advective effect on the annual range of sea surface temperature. *Geophysical Research Letters*, **32**, L24604, DOI: 10.1029/2005GL024493.
- Lukas, T., and Lindstrom, E., 1991. The mixed layer of the western equatorial Pacific Ocean. *Journal of Geophysical Research*, **96**: 3343-3357.
- Luo, J. J., Zhang, R. C., Behera, S. K., Masumoto, Y., Jin, F. F., Lukas, R., and Yamagata, T., 2010. Interaction between El Niño and Extreme Indian Ocean Dipole. *Journal of Climate*, **23**: 726-742, DOI: <http://dx.doi.org/10.1175/2009JCLI13104.1>.
- Masson, S., Luo, J. J., Madec, G., Vialard, J., Durand, F., Gualdi, S., Guilyardi, E., Behera, S., Delecluse, P., Navarra, A., and Yamagata, P., 2005. Impact of barrier layer on winter-spring variability of the southeastern Arabian Sea. *Geophysical Research Letters*, **32**, L07703, DOI: 10.1029/2004GL021980.
- Monterey, G., and Levitus, S., 1997. Seasonal variability of mixed layer depth for the world ocean. *NOAA Atlas NESDIS 14*. U.S. Gov. Printing Office, Washington D.C., 96pp.
- Morioka, Y., Tozuka, T., and Yamagata, T., 2010. Climate variability in the Southern Indian Ocean as revealed by self-organizing maps. *Climate Dynamics*, **35**: 1059-1072, DOI: 10.1007/s00382-010-0843-x.
- Morioka, Y., Tozuka, T., and Yamagata, T., 2011. On the growth and decay of the subtropical dipole mode in the South Atlantic. *Journal of Climate*, **24**: 5538-5554, DOI: 10.1175/2011JCLI4010.1.
- Murtugudde, R., McCreary, J. P., and Busalacchi, A. J., 2000. Oceanic processes associated with anomalous events in the Indian Ocean with relevance to 1997–1998. *Journal of Geophysical Research*, **105**: 3295-3306.
- Praveen Kumar, B., Vialard, J., Lengaigne, M., Murty, V. S. N., and McPhaden, M. J., 2012. TropFlux: air–sea fluxes for the global tropical oceans-description and evaluation. *Climate Dynamics*, **38**: 1521-1543, DOI: 10.1007/s00382-011-1115-0.
- Qiu, B., 2000. Interannual variability of the Kuroshio extension system and its impact on the wintertime SST field. *Journal of Physical Oceanography*, **30**: 1486-1502.
- Qiu, Y., Cai, W., Li, L., and Guo, X., 2012. Argo profiles variability of barrier layer in the tropical Indian Ocean and its relationship with the Indian Ocean Dipole. *Geophysical Research Letters*, **39**, L08605, DOI: 10.1029/2012GL051441.
- Rao, R. R., and Sivakumar, R., 1999. On the possible mechanisms of the evolution of a mini-warm pool during the pre-summer monsoon season and the onset vortex in the southeastern Arabian Sea. *Quarterly Journal of the Royal Meteorological Society*, **125**: 787-809.
- Rao, R. R., and Sivakumar, R., 2003. Seasonal variability of sea surface salinity and salt budget of the mixed layer of the north Indian Ocean. *Journal of Geophysical Research*, **108** (C1), 3009, DOI: 10.1029/2001JC000907.
- Reynolds, R. W., Rayner, N. A., Smith, T. M., Stokes, D. C., and Wang, W., 2002. An improved *in situ* and satellite SST analysis for climate. *Journal of Climate*, **15**: 1609-1625.
- Saji, N. H., Goswami, B. N., Vinayachandran, P. N., and Yamagata, T., 1999. A dipole mode in the Tropical Indian Ocean. *Nature*, **401**: 360-363.
- Sharma, R., Agarwal, N., Momin, I. M., Basu, S., and Agarwal, V. K., 2010. Simulated sea surface salinity variability in the Tropical Indian Ocean. *Journal of Climate*, **23**: 6542-6554, DOI: <http://dx.doi.org/10.1175/2010JCLI3721.1>.
- Shenoi, S. S. C., Shankar, D., and Shetye, S. R., 1999. On the sea surface temperature high in the Lakshadweep Sea before the onset of the southwest monsoon. *Journal of Geophysical Research*, **104** (C7): 15703-15712.
- Shenoi, S. S. C., Shankar, D., and Shetye, S. R., 2004. Remote forcing annihilates barrier layer in southeastern Arabian Sea. *Geophysical Research Letters*, **31**, L05307, DOI: 10.1029/2003GL019270.
- Shetye, S. R., Gouveia, A. D., Shenoi, S. S. C., Michael, G. S., Sundar, D., Almeida, A. M., and Santanam, K., 1991. The coastal current off western India during the northeast monsoon. *Deep-Sea Research (Part A)*, **38**: 1517-1529.
- Thadathil, P., and Gosh, A. K., 1992. Surface layer temperature inversion in the Arabian Sea during winter. *Journal of Oceanography*, **48**: 293-304.
- Vialard, J., and Delecluse, P., 1998a. An OGCM study for the TOGA decade. Part I. Role of salinity in the physics of the western Pacific fresh pool. *Journal of Physical Oceanography*, **28**: 1071-1088.
- Vialard, J., and Delecluse, P., 1998b. An OGCM study for the TOGA decade. Part II. Barrier-layer formation and variability. *Journal of Physical Oceanography*, **28**: 1089-1106.
- Wang, B., Wu, R., and Li, T., 2003. Atmosphere–warm ocean interaction and its impact on Asian–Australian monsoon variation. *Journal of Climate*, **16**: 1195-1211.
- Webster, P. J., Moore, A. M., Loschnigg, J. P., and Leben, R. R., 1999. Coupled ocean–atmosphere dynamics in the Indian Ocean during 1997–98. *Nature*, **401**: 356-360.
- Xie, S. P., Annamalai, H., Schott, F. A., and McCreary, J. P., 2002. Structure and mechanisms of South Indian Ocean climate variability. *Journal of Climate*, **15**: 864-878.
- Xie, S. P., Xu, H., Saji, N. H., Wang, Y., and Liu, W. T., 2006. Role of narrow mountains in large-scale organization of Asian monsoon convection. *Journal of Climate*, **19**: 3420-3429.
- Yamagata, T., Behera, S. K., Rao, S. A., Guan, Z., Ashok, K., and Saji, H. N., 2002. The Indian Ocean Dipole: a physical entity. *CLIVAR Exchanges*, **24**: 15-18.
- Yamagata, T., Behera, S. K., Rao, S. A., Guan, Z., Ashok, K., and Saji, H. N., 2003. Comments on ‘Dipoles, temperature gradient, and tropical climate anomalies’. *Bulletin of the American Meteorological Society*, **84**: 1418-1422.
- Yu, L., Jin, X., and Weller, R. A., 2008. Multidecade global flux datasets from the objectively analyzed air–sea fluxes (OAFlux) project: Latent and sensible heat fluxes, ocean evaporation, and related surface meteorological variables. *Woods Hole Oceanographic Institution OAFlux Project Technical Report (OA-2008-01)*, Woods Hole. Massachusetts. 64pp.
- Zheng, X. T., Xie, S. P., Vecchi, G. A., Liu, Q., and Hafner, J., 2010. Indian Ocean Dipole response to global warming: analysis of ocean–atmospheric feedbacks in a coupled model. *Journal of Climate*, **23**: 1240-1253.

(Edited by Xie Jun)